

Indexing of CNN Features for Large Scale Image Search

Ruoyu Liu, Yao Zhao, Shikui Wei, Zhenfeng Zhu, Lixin Liao, Shuang Qiu

Institute of Information Science, Beijing Jiaotong University, Beijing, 100044, China

Beijing Key Laboratory of Advanced Information Science and Network Technology, Beijing, 100044, China

{12112062, yzhao, shkwei, zfzhu, 14125143, 14120332}@bjtu.edu.cn

Abstract

Convolutional neural network (CNN) feature that represents an image with a global and high-dimensional vector has shown highly discriminative capability in image search. Although CNN features are more compact than most of local representation schemes, it still cannot efficiently deal with large-scale image search issues due to its non-negligible computational cost and storage usage. In this paper, we propose a simple but effective image indexing framework to improve the computational and storage efficiency of CNN features. Instead of projecting each CNN feature vector into a global hashing code, the proposed framework adapts Bag-of-Word model and inverted table to global feature indexing. To this end, two strategies, which are based on semantic information associated with CNN features, are proposed to convert a global vector to one or several discrete words. In addition, several strategies for compensating quantization error are fully investigated under the indexing framework. Extensive experimental results on two public benchmarks show the superiority of our framework.

1. Introduction

Image search [7, 43] aims to find out relevant images of a user's query from mass data, which is the fundamental problem in many real-world scenarios. In the last two decades, the main effort focuses on improving the searching accuracy and efficiency. In essence, the searching accuracy is closely related to the features extraction, whereas the searching efficiency is depended mainly on the indexing structure.

To represent the image content accurately, various feature extraction schemes have been reported [22, 21, 34, 9, 30, 17, 37], which can be coarsely separated into two groups: global features and local features. Global features such as Color Histogram [22], Tamura [21] and Moment Invariant [34], are often the statistics of images' color, textual or shape information, where each image is described as a single and short vector. Generally, this kind of feature is compact and efficient for performing image search task.

However, they cannot handle some complex image transformations like scale and layout changes, since they can only capture low-level information in images. In contrast, local features, e.g., SIFT [9] and SURF [17], describe an image with a set of local descriptors and have a better discriminative capability of different contents. However, their shortcoming is that the amount of local features extracted from even a small image dataset is huge. When the dataset is large scale, image search system based on local features will result in insufferable storage usage and computational cost.

To speed up the searching process, various indexing schemes have also been studied sufficiently. For most of division based indexing structures such as R-tree [5], M-tree [36] and inverted table [26], they commonly divide the whole database into a series of non-overlapping partitions. Since only a small part of the whole dataset will be compared with the query image, the searching efficiency is improved significantly. Another bunch of indexing schemes is hashing based methods [33, 47, 12, 27, 28, 23, 41, 49, 29], which learns a set of hash functions to map images from their original feature space into a distance-preserving binary space. Since fast bitwise operation can be employed to compare two binary codes, the searching efficiency can be boosted greatly.

While many image search frameworks have been proposed, the current state-of-the-art is still based on bag-of-words (BoW) model and inverted tables [26, 10, 14, 4]. However, this framework is only suitable for small- or medium-scale image search scenarios. When the database is large-scale, both the computational and storage efficiency will deteriorate sharply. Recently, global feature learning technique based on deep learning (DP) is becoming popular. Instead of representing only the low-level visual information, this kind of feature encodes the high-level semantic meanings of image into a high-dimensional vector. For example, the global feature learned by Convolution Neural Networks (CNN) [6], called CNN feature, consists of thousands of variables (e.g., 1000D or 4098D). However, although it is extremely discriminative and also more com-

pact than most of local representation schemes, the computational and storage cost are non-negligible when image dataset is huge. Therefore, it is necessary for large-scale applications to build an efficient indexing structure.

In this paper, we attempt to develop a new image indexing framework on basis of CNN features. Instead of projecting each CNN vector from the original feature space into a binary space, we adapt BoW model and inverted table to dealing with high-dimensional global features. The key contributions and novelties are summarized as follows: (1) A simple but effective image indexing framework is proposed to improve computational and storage efficiency. (2) Several strategies are proposed to decompose CNN features to visual words. Since BoW model is tailored to local features, we need to design some strategies to map global features into visual words. To this end, two visual dictionary constructing methods, which depend on semantic information underlying CNN features, are proposed. (3) Several strategies are proposed to compensate the information loss caused by CNN feature decomposition. Commonly, a CNN feature is replaced with only one visual word, which will lead to large information loss. To address this issue, multiple link and multiple assignment strategies are applied in this paper. Moreover, a novel joint indexing scheme, which combines a series light-weight inverted tables, is proposed to improve the search accuracy. Extensive experimental results on two public benchmarks show the superiority of our framework.

2. Related Work

In this section, we firstly give the introduction about Convolutional Neural Network (CNN), which is used in this paper for learning the global image features. Then we give a brief review of existing image indexing structure based on the inverted table.

2.1. Convolutional Neural Network

Deep learning (DL) has drawn much attention from both academic and industry communities due to its excellent capability in representing image content [3, 8, 46]. *G.E.Hinton* etc. report a pioneering work on deep learning in [16], which includes two key steps. First, neurons are built layer by layer, which trains a single layer each time. Then “Wake-Sleep” algorithm is performed to optimize the whole network. By adjusting the weights in the network, “Wake-Sleep” algorithm makes sure that the final output represents the raw input as much as possible. *X.Wang* etc. [45] developed the DeepID, whose accuracy of face recognition is more than 99%, and identified faces are even more precise than the naked eye. *K.Alex, S.Hya and E.H.Geoffrey* [6] win the top-5 test error rate of 15.3% in the ILSVRC-2012 competition by using deep convolutional neural networks. In a word, deep learning has set off

a wave of artificial intelligence.

In this work, we extract the global image features by using the deep convolutional neural networks toolkit, named Caffe [44]. The network of Caffe takes an image as the input and generates a feature vector of 4096 or 1000 dimensions as output. The architecture of the network originated from [6] contains eight learned layers including five convolutional and three fully-connected layers. The whole architecture is illustrated in Fig. 1. As shown in Fig. 1, we use an image with single channel as the input. Every convolutional layer contains different size and numbers of the convolutional kernels. The kernels are $11 \times 11 \times 96$, $5 \times 5 \times 256$, $3 \times 3 \times 384$, $3 \times 3 \times 384$, $3 \times 3 \times 256$ in order. The overlapping pooling is acting behind the first, second and fifth convolutional layers. Dropout [15], which is a technology of preventing co-adaptation of feature detectors, is used in the sixth, seventh and eighth fully-connected layers. We adopt the output of the sixth layer as the CNN features, which is a feature vector of 4096 dimensions.

2.2. Inverted Table

The inverted table is initially used to index text documents in text retrieval area. For facilitating the image matching on basis of local features, *Sivic* [26] etc. extend this technique to image indexing via the BoW model [26, 10, 14, 40]. The key idea of BoW model is to construct a visual dictionary and represent each image with an orderless collection of visual words in the dictionary. In this way, the representation of an image is similar to a text document, and the inverted table can directly employed to index images. The basic framework of inverted table is shown in Fig. 2, which depends on a fixed visual dictionary. For each visual word, a list is built, in which the ID information of images that contains the visual word is inserted. In the search phase, a voting process is performed to measure the similarity between query and database images.

A lot of work has been done to improve the performance of inverted table. To effectively construct the visual dictionary, some fast clustering methods have been proposed to decrease the time cost of training dictionary [11, 35, 39, 18]. In addition, binary embedding techniques have also been proposed to improve the search accuracy by adding additional information to the inverted table [19, 18, 20, 13, 42, 32, 31, 48].

The traditional BoW model + inverted table framework is tailored for local image features. However, when image is represented by a single global feature, traditional inverted table is no longer suitable for indexing images due to the large quantization error. Therefore, we have to take some strategies to adapt the traditional indexing scheme for fitting the global features. Details are given in section 4.

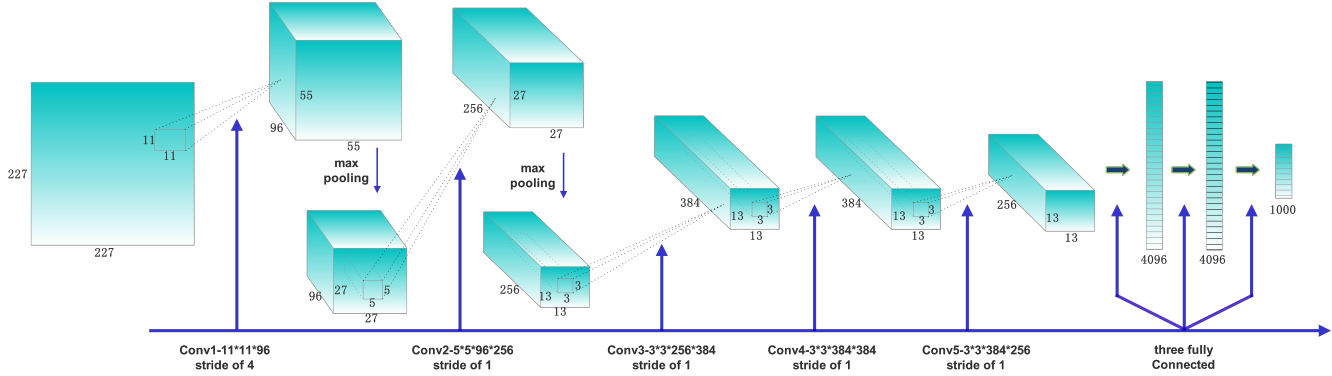


Figure 1. Illustration of Convolutional Neural Network model used in this paper.

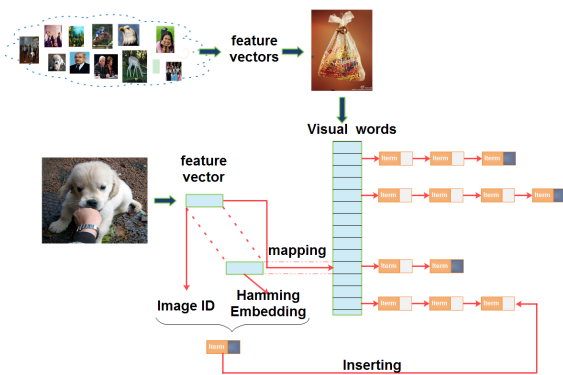


Figure 2. The basic framework of inverted table.

3. Overview of the Indexing Framework

3.1. Problem Description

Suppose we have a set of N images described by D -dimensional CNN features: $X = \{x_1, \dots, x_N\}$, where $x_i \in R^D, i = 1, \dots, N$. Our goal is to develop an effective and efficient image indexing framework so as to perform fast and accurate image search. A straightforward solution is to index the CNN features by employing hashing functions. In essence, hashing based schemes are to project images from their original feature space into a distance-preserving binary space. However, hashing global features of images will lead to large loss of discriminative capability. Therefore, we need to design a new image indexing framework. In this paper, we attempt to design the global feature indexing framework by borrowing some ideas from image indexing of local features. In classical local feature based image indexing framework, the key techniques are BoW model and inverted table. To adapt these techniques to global features, two main problems should be addressed.

Problem 1: How to convert a high-dimensional global feature into a set of visual words?

For traditional BoW model + inverted table framework, local features of an image are first quantized into visual words, and then these visual words are indexed into inverted table. That is, this framework is tailored for local features. Nevertheless, CNN features are global features, we need to design some new strategies to map global features into visual words.

Problem 2: How to avoid large loss of discriminative capability when mapping global features into visual words?

When we convert global features into visual words, there exists quantization error between feature and visual word. Especially, when a global feature is mapped to only one visual word, the quantization error is larger. It clearly decreases the discriminative capability of features, since dissimilar images may be described by the same visual word. Therefore, additional information and strategies need to be introduced to enhance the discriminative capability of global features when indexed by inverted table.

3.2. Solution Overview

To solve problem 1, we propose two strategies to map a global CNN feature into one or several visual words. The first strategy depends on semantic information of different components in global vector. Since CNN features belong to a relative high-level feature, each component is of some specific semantic content. Therefore, each component can be treated as corresponded to a virtual concept word. In this way, a dictionary with a fixed size, which is equal to the length of CNN vector, can be constructed. In this situation, a CNN vector can be treated as a term frequency vector against the dictionary. For the second strategy, we directly employ the traditional methods to learn dictionaries. In our scheme, the Product Quantization (PQ) is used to learn visual dictionaries due to its low cost in computation and memory usage.

To solve problem 2, four compensation strategies are proposed. First, we apply multiple link and multiple assignment strategies to reduce the quantization error. Since one image is represented by only one CNN feature, quantizing the CNN feature into only one word will lead to large information loss. Therefore, we employ multiple link strategy to index each database CNN feature to several inverted list in the indexing stage. Meanwhile, we also use multiple assignment strategy to map each query CNN feature into several visual words in the querying stage. For the third strategy, we propose to construct a series light-weight inverted tables for the database so as to alleviate the missed matches. To further reduce quantization error, binary embedding techniques are also introduced into the image indexing framework. Besides of visual words, each CNN feature is also associated with a compact binary code. In the querying stage, the returned images for a query will be further checked by calculating the hamming distance between query image and any returned image. If the distance is lower than a fixed threshold T , the returned image is reserved, otherwise ignored [38].

The proposed image indexing framework is related to many existing techniques, such as BoW model, inverted table, binary embedding schemes. However, the key difference lies in that these related techniques are tailored to local feature based image search framework while our scheme adapts them to index global features. For example, the traditional inverted table is used in BOW model to index local features, in which each image is represented by a set of local features. While in our scheme, each image is described by only a single CNN feature and the original inverted table must be adapted to index global features.

Compared with the brute force (BF) search of CNN features, our schemes is clearly faster since the searching scope is greatly narrowed against the inverted table. More importantly, the memory usage is significantly reduced due to the compact description of visual words and embedding codes.

4. Details of the Proposed Framework

In this section, we introduce the details of the proposed indexing framework. We firstly give the overview of the whole schemes, where the common components are discussed shortly. Then, separate techniques used in our proposed methods are given in details.

4.1. Overview of the Indexing Framework

The final goal of our work is to use the inverted table to perform fast and accuracy image retrieval on CNN features. To this end, visual dictionaries are needed to be constructed for quantizing the CNN features firstly. In our indexing framework, several dictionary construction strategies are proposed, we discuss it latter. After a dictionary with K visual words $C = \{c_1, \dots, c_K\}$ is constructed, the

next step is to link the images to the corresponding position of the inverted table. For local feature based image indexing [38], since each local feature must be indexed to inverted table, most of existing schemes commonly link each local feature to only one visual word so as to avoid large storage usage. We call the link rule as single link (SL). In our scenario, each image is described by one vector. If each image is linked to only one visual word, the probability that two similar images that link to the same word will be relatively small. Therefore, in all our schemes, each image is linked to its S nearest words in the indexing stage, and we call the link rule as multiple link (ML).

In the search phase, the query image x_q can be assigned to the nearest visual word and be linked to corresponding list. We name the process that assign an query image to only one visual word as single assignment (SA). As in [38], we can also assign a global CNN feature to W visual words and return all images linked to these words. Similar to [38], we call this process as multiple assignment (MA). After that, a voting process is performed according to the frequency that an image is returned. Notice that SL and SA are called hard assignment, and ML and MA are called soft assignment in [25, 38].

4.2. CNN Feature as Term Frequency Vector

The key for constructing an inverted table is to build a dictionary and to convert global features into a set of words in the dictionary. Since each component of the CNN feature vector is of some semantic content, we can treat each dimension as corresponded to a virtual concept word. Therefore, a dictionary whose size is equal to length of feature vector is naturally built as shown in Fig. 3. Since term frequency is the probability of each word appearance in a document, the CNN feature vector is translated into a term frequency (probability) vector. In our scheme, given a CNN feature vector $x = (x^1, \dots, x^D)^T$, we further deal with each component by using the following softmax function:

$$\sigma(x^i)_i = \frac{e^{x^i}}{\sum_{j=1}^D e^{x^j}} \quad (1)$$

In this way, a CNN feature vector can be translated to a histogram $\sigma(x) = (\sigma(x^1)_1, \dots, \sigma(x^D)_D)^T$, where each bin indicates the probability that corresponding word appears in the image. If without any post-processing step, D items will be inserted into the inverted table with D lists, which will lead to a large memory cost. To avoid this problem, only the words corresponding to top S bin values are taken into account. It is reasonable, since the top value bins describe the main content of the image.

Since too many CNN features are linked to a single position, the quantization error is big. To further improve the search accuracy, binary embedding codes of CNN features

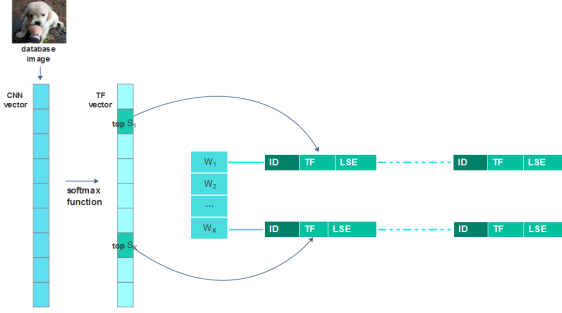


Figure 3. Illustration of TF+LSE indexing structure.

are calculated and introduced into the inverted table structure. Assume image x is linked to the virtual visual word c and we want to generate a binary code with length L . First, we need to partition x and c into L parts with equal length. The following formulates the partitioning process:

$$x = (x_{(1)}, \dots, x_{(L)})^T \quad (2)$$

$$c = (c_{(1)}, \dots, c_{(L)})^T \quad (3)$$

where $x_{(i)} = (x_{(i-1) \times (D/L) + 1}, \dots, x_{i \times (D/L)})^T$ and $c_{(i)} = (c_{(i-1) \times (D/L) + 1}, \dots, c_{i \times (D/L)})^T$. Then the binary code $l = (l^1, \dots, l^L)^T$ is calculated as follows:

$$\begin{cases} l^{(i)} = 1 & \text{if } \text{mean}(x_{(i)}) \geq \text{mean}(c_{(i)}) \\ l^{(i)} = 0 & \text{if } \text{mean}(x_{(i)}) < \text{mean}(c_{(i)}) \end{cases} \quad (4)$$

In this scheme, since D visual words are virtual words, we randomly generate D -dimensional vectors to represent these virtual words so as to calculate the binary code. Experiments show that it has no effect on the retrieved results. We call this scheme as “TF+LSE” for short. For memory saving, the binary embedding codes are stored in bits.

4.3. Index Large Scale of CNN Features

Using the above-mentioned method, only a small-scale dictionary with thousands of virtual words can be used to construct the inverted table. However, when the image database is very large-scale, both the effectiveness and efficiency of the indexing structure will be deteriorated. Therefore, it is necessary to build a large-scale visual dictionary. Taking into account the efficiency in training and mapping, we employ product quantization(PQ) [38, 18] method to learn a large-scale visual dictionary from a training set of global CNN features. In particular, the CNN features in training dataset is firstly partitioned into M segments with equal length, i.e., $x = (x_{(1)}, \dots, x_{(M)})$. Then k-means clustering method is performed on each vector segment to get a sub-codebook $C^{(i)}$ with K sub-words. By using the Cartesian product, all the M sub-dictionaries (or sets) are combined to construct a final visual dictionary with K^M visual

words, i.e., $C = C^{(1)} \times \dots \times C^{(M)}$. Once we have built the large-scale dictionary, an inverted table can be constructed against it. Similarly, binary embedding codes are associated with the inverted table by using the Eq. 4. We call this method “PQ+LSE” for short, whose framework is shown in Fig. 4.

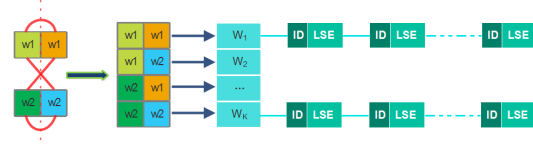


Figure 4. Illustration of PQ+LSE indexing structure

4.4. Randomly Permutation of CNN Feature

For CNN features, each component is of some specific semantic content. In addition to occurrence probability of semantic contents, the CNN vector also indicates the co-occurrence correlation among all components. However, when PQ technique is applied, the CNN feature vector is roughly separated into several segments, and each segment is assumed to be independent with others. Therefore, the co-occurrence semantic correlation among components in different segments is destroyed. For example, suppose the 2nd and 5th elements of CNN feature vector are relative with the similar semantic content, then we can say that they have strong co-occurrence correlation. If they are separated into different groups, they are thought to be independent with each other and the correlation is destroyed.

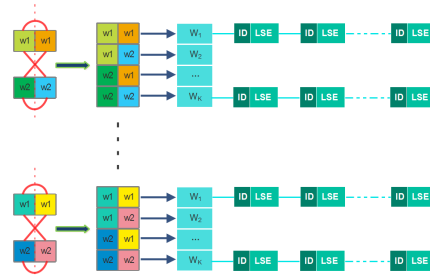


Figure 5. Illustration of M-PQ+LSE indexing structure.

To address this issue, we obtain a series of permutations of the CNN vector’s components by randomly rearranging the order of components. For each permutation, we use it to pre-process both training and database CNN features, and build an inverted table via PQ+LSE scheme. Consequently, we can build a series of independent inverted tables as shown in Fig. 5. In the search phase, the search process is independently performed on each of permutation-dependent inverted tables, and the scores from different inverted tables but voting to a certain image are fused together

by using linear combination. We call this scheme as “M-PQ+LSE”.

4.5. Combination

In the above-mentioned schemes, the key is to construct different visual dictionaries with different strategies so as to compensate the large quantization error and decrease the probability of missed matches. Therefore, combining different schemes is expected to achieve a better result. By combining the “TF+LSE” and “PQ+LSE” schemes, we can build a new indexing structure with 2 inverted tables as shown in Fig. 6. We call this scheme as “TF+PQ+LSE”.

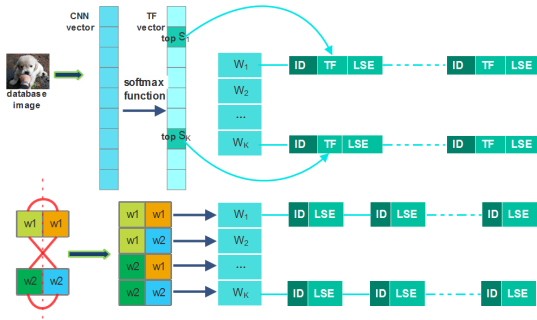


Figure 6. Illustration of TF+PQ+LSE indexing structure

5. Experiments

We represent the experimental results and analysis in this section. To validate the effectiveness of our proposed schemes, we perform our experiments on two landmark datasets. Besides, a large scale dataset is added into the two landmarks as the distractor set to test the performance of the proposed schemes on big data environment.

5.1. Experimental Setup

In our experiment, **Holiday** and **Oxford** are employed as two landmark datasets. When testing on large scale datasets, **Flickr1M** is added into each landmark as a distractor set. All the CNN features are extracted by using Caffe [44] toolkit with default model.

Holiday [19] is an image dataset containing some personal holiday photos. It contains 1491 images in total separated by 500 groups, where each group represents a specific scene or object. The first image of each group is the query image and all images of the group are the correct retrieval results.

Oxford [24] is a building datasets consists of 5062 images downloaded from Flickr by searching for particular Oxford landmarks. The dataset is manually annotated to generate a comprehensive ground truth for 11 different

landmarks, each represented by 5 possible queries. That gives 55 query images in total.

Flickr1M [1] dataset contains 1,197,398 images downloaded from Flickr. In our experiments, we randomly select 900,000 images as the distractor set and treat the others as training set.

We use Mean Average Precision (**MAP**) as the accuracy measure. Average Precision (AP) [38] is corresponded to the ranks of the ground-truth in the returned list. After getting APs of all queries, the mean value is calculated as the final score.

5.2. Comparison Methods

Four schemes proposed in Section 4 are compared in accuracy, speed and storage cost. Besides, two baseline are added into comparison. One of them is the brute-force (BF) scheme, which uses CNN features to perform search directly. Another is Locality Sensitive Hashing (LSH) [33], which is a famous hashing scheme.

5.3. Effect of Key Parameters

There are five main factors that affect the schemes, the binary code length L , the link number S , the assignment number W , the distance threshold T and the permutation number R . To test the sensitivity of the proposed schemes to these factors, we perform experiments on the two landmarks without distractor set. We firstly give the results on **Holiday** dataset. Notice that M-PQ+LSE and TF+PQ+LSE schemes are based on TF+LSE and PQ+LSE, so it is enough to evaluate the sensitivity of parameters on TF+LSE and PQ+LSE schemes.

The effect of factor L on Holiday dataset is illustrated in Fig. 7. Clearly, a medium length of binary code achieves the best performance. In fact, it is reasonable to get this conclusion since a medium binary code can better balance missed matches and false matches. In the following experiments, we set $L = 512$ for all schemes.

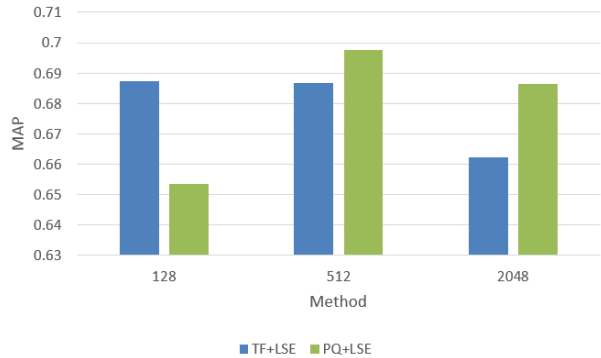


Figure 7. The sensitivity of factor L on **Holiday** dataset.

To test the sensitivity of factor T , we also carry out a

group of experiments on holiday dataset. The experimental results are shown in Fig. 8. When the threshold is below to 170, the MAP score increases with the threshold. When the threshold exceeds 170, the increases trend to be smooth. This is because when the threshold is small, many correct results are wrongly rejected since the binary code is just a similar representation of visual feature. In contrast, when the threshold is too large, it also lose effect since too many wrong results are reserved. Empirically, when the threshold is about 30% of code length, the result is the best. The experiments has validated this conclusion.

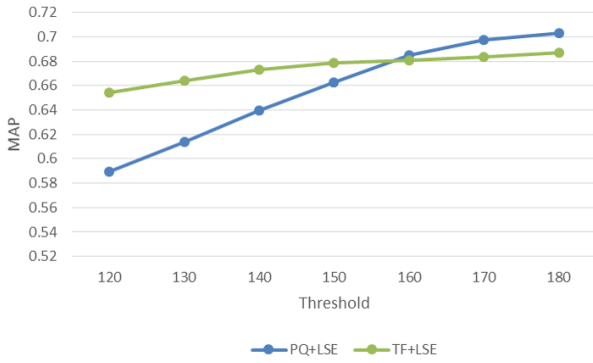


Figure 8. The sensitivity of factor T on **Holiday** dataset.

For the factors S and W in PQ+LSE, there is strong correlation between multiple link and multiple assignment. We can observe that when $S = W$, the performance is best. This is because when $S = W$, the probability of finding the most correct images is biggest. When $S > W$, it is more possible for the query to lose the most correct images. In contrast, when $S < W$, too wrong images will be returned. Due to the page limitation, we give the experimental results in the supplemental material to show this conclusion. Here, we force the value of S to be equal to W . The experimental results are illustrated in Fig. 9. Clearly, the bigger of S and W , the better of search accuracy, while the search time increases linearly with the factors as shown in Fig. 10. In fact, the accuracy improvement trends to be smooth when S and W go up to a certain value. As shown in Fig.9, when the values of S and W are bigger than 40, the value of MAP tends to be stable. This means that we can significantly improve search accuracy with relative small time cost.

The sensitivity of R is tested on M-PQ+LSE scheme. The MAP score change curve with R is shown in Fig. 11. The results show that the score of MAP increases with R . When $R < 15$ the increase is obvious, while when $R > 25$ the score tends to be equal. The time cost change curve is shown in Fig. 12, increases linearly. This is because for each iteration, it performs the same search process. If two elements of CNN feature have co-occurrence correlation, there is still a big probability that they are separated into the

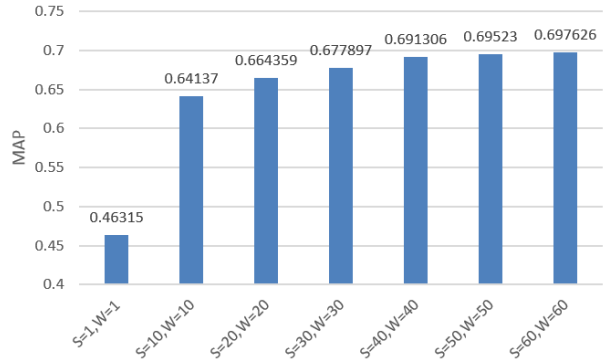


Figure 9. The accuracy sensitivity of factor S and W on **Holiday** dataset.

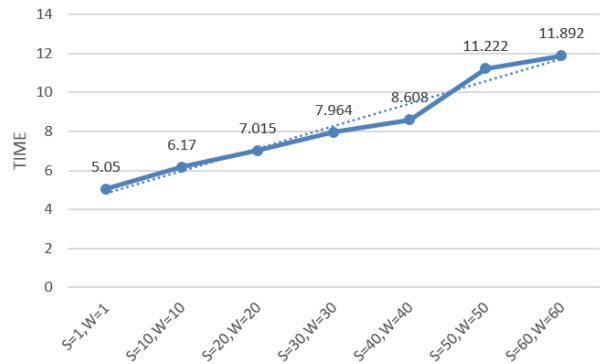


Figure 10. The speed sensitivity of factor S and W on **Holiday** dataset.

same group when PQ is performed so that to enhance the correlation.

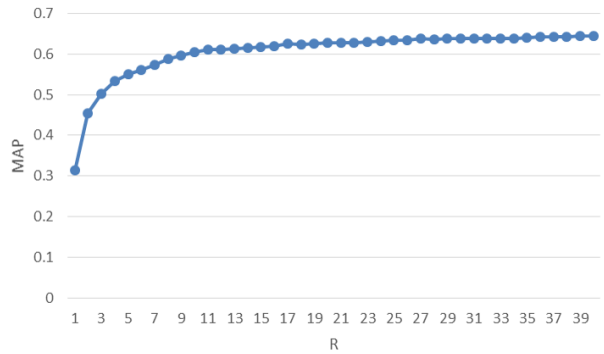


Figure 11. The accuracy sensitivity of factor R on **Holiday** dataset.

The conclusion got from **Oxford** dataset shown in supplemental material.

5.4. Comparison of Different Schemes

In this subsection, the experimental results of various schemes are compared together. We carry out a series of ex-

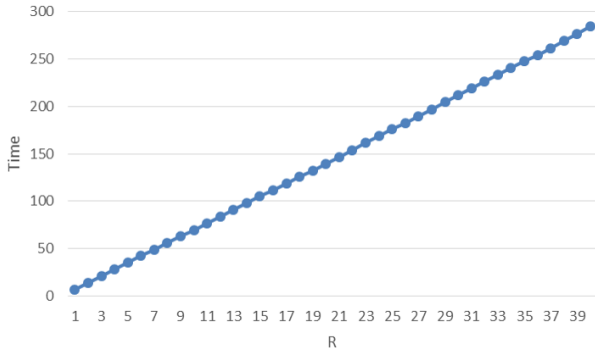


Figure 12. The speed sensitivity of factor R on **Holiday** dataset.

periments on both landmarks with and without the distractor set. For all proposed schemes, the factors are set the best according to the conclusion in Section 5.3. For TF+PQ+LSE, we combine the results of TF+LSE and PQ+LSE. Besides, a baseline of brute-force search is added for comparison.

The evaluation of image search accuracy on **Holiday** dataset are shown in Table 1. Clearly, brute-force search outperforms all our indexing schemes. This is not surprising since the quantization error unavoidably decreases the discriminative capability of the original CNN features. In fact, using the proposed indexing schemes, we can also achieve excellent performance. For example, TF+PQ+LSE scheme obtains a high accuracy of 0.728610. Interestingly, there are no remarkable performance deterioration after introducing a large distractor set. For M-PQ+LSE, the value is when S and W both equal to 1. Increasing the value of these two parameters can improve the accuracy of this scheme.

Table 1. Evaluation of searching accuracy on **Holiday**.

Method	Dataset	
	Holiday	Holiday+Flickr1M
BF (baseline)	0.788241	0.788205
TF+LSE	0.683791	0.683790
PQ+LSE	0.702020	0.701414
M-PQ+LSE	0.644091	0.643276
TF+PQ+LSE	0.728903	0.728610

In our work, the main advantages of the proposed indexing framework lie in high efficiency and less storage usage. As shown in Table 2, all our schemes significantly improve the searching efficiency in a large-scale environment. More importantly, the searching time is sub-linear with the growth of database. For example, the searching time is only doubled for PQ+LSE scheme, while the database has been increased about a thousand-fold. Notice that when the landmark is used without the distractor set, we can see that BF is not the worst. However, it is reasonable. Since the volume of Holiday dataset is 1491, BF needs only to search

1491 CNN vectors to get the results. Nevertheless, PQ+LSE needs to search two codebooks with 1000 words and to find the cell ID for each in inverted table. Therefore, the initial step is nontrivial for small dataset.

Table 2. Evaluation of Search Time on **Holiday**. (Unit: s)

Method	Dataset	
	Holiday	Holiday+Flickr1M
BF (baseline)	7.005	4616.796
TF+LSE	4.387	34.373
PQ+LSE	10.787	22.987
M-PQ+LSE	284.212	1165.360
TF+PQ+LSE	15.174	57.360

The memory usage of each scheme when performing search on **Holiday** is shown in Table 3. For small dataset, since most of memory is used to store the visual dictionaries, the proposed schemes take more space. When the dataset is huge, the memory usage of all our scheme will far lower than the BF scheme. For example, TF+PQ+LSE only takes 4330.12M memory space, compared to 14085.80M of BF.

Table 3. Evaluation of Storage Usage on **Holiday**. (Unit: MB)

Method	Dataset	
	Holiday	Holiday+Flickr1M
BF (baseline)	23.30	14085.80
TF+LSE	65.23	806.80
PQ+LSE	21.43	3523.32
M-PQ+LSE	628.87	2963.46
TF+PQ+LSE	86.66	4330.12

We supply the experimental results on **Oxford** dataset in the supplemental material. Besides, comparison results with another baseline LSH, is also given there.

6. Conclusion

In this paper, we propose a simple but effective image indexing framework to improve computational and storage efficiency of global CNN features. Inspired by local feature indexing methods, we adapt the traditional BoW model + inverted table framework to global feature indexing. Fully exploring the semantic information underlying components of CNN vector, we propose two visual dictionary construction methods to map global CNN features to discrete words. To alleviate the quantization error, four compensation strategies are fully investigated in our indexing framework. Extensive experimental results shown that the proposed framework significantly improves computational and storage efficiency with an acceptable loss of precision.

References

- [1] <http://www.multimedia-computing.org/wiki/Flickr1M>. 6
- [2] <http://www.flickr.com/>. 13
- [3] A.Babenko, A.Slesarev, A.Chigorin, and V.Lempitsky. Neural codes for image retrieval. In *ECCV*, pages 584–599. Springer, 2014. 2
- [4] A.Babenko and V.Lempitsky. The inverted multi-index. In *CVPR*, pages 3069–3076. IEEE, 2012. 1
- [5] A.Guttman. *R-trees: a dynamic index structure for spatial searching*, volume 14. 1984. 1
- [6] A.Krizhevsky, I.Sutskever, and G.E.Hinton. Imagenet classification with deep convolutional neural networks. In *NIPS*, pages 1097–1105. 1, 2
- [7] A.Mishra, K.Alahari, and C.Jawahar. Image retrieval using textual cues. In *ICCV*, pages 3040–3047, 2013. 1
- [8] A.S.Razavian, H.Azizpour, J.Sullivan, and S.Carlsson. CNN features off-the-shelf: an astounding baseline for recognition. In *CVPRW*, pages 512–519. IEEE, 2014. 2
- [9] D.G.Lowe. Distinctive image features from scale-invariant keypoints. *IJCV*, 60(2):91–110, 2004. 1
- [10] D.Nister and H.Stewenius. Scalable recognition with a vocabulary tree. In *CVPR*, volume 2, pages 2161–2168, 2006. accessed from <http://www.vis.uky.edu/~stewe/ukbench/>. 1, 2, 14
- [11] D.Nister and H.Stewenius. Scalable recognition with a vocabulary tree. In *CVPR*, volume 2, pages 2161–2168, 2006. 2
- [12] D.Zhang, J.Wang, D.Cai, and J.Lu. Self-taught hashing for fast similarity search. In *SIGIR*, pages 18–25, 2010. 1
- [13] D.Zhuang, D.Zhang, J.Li, K.Lv, and Q.Tian. Hamming embedding with fragile bits for image search. In *ICIP*, pages 5721–5725, 2014. 2
- [14] E.Nowak, F.Jurie, and B.Triggs. Sampling strategies for bag-of-features image classification. In *ECCV*, pages 490–503. 2006. 1, 2
- [15] G.E.Hinton, N.Srivastava, A.Krizhevsky, I.Sutskever, and R.R.Salakhutdinov. Improving neural networks by preventing co-adaptation of feature detectors. *arXiv preprint arXiv:1207.0580*, 2012. 2
- [16] G.E.Hinton and R.R.Salakhutdinov. Reducing the dimensionality of data with neural networks. *Science*, 313(5786):504–507, 2006. 2
- [17] H.Bay, T.Tuytelaars, and L. Gool. Surf: Speeded up robust features. In *ECCV*, pages 404–417. 2006. 1
- [18] H.Jegou, M. Douze, and C. Schmid. Product quantization for nearest neighbor search. *TPAMI*, 33(1):117–128, 2011. 2, 5
- [19] H.Jegou, M.Douze, and C.Schmid. Hamming embedding and weak geometric consistency for large scale image search. In *ECCV*, pages 304–317. Springer, 2008. accessed from <http://lear.inrialpes.fr/people/jegou/data.php>. 2, 6
- [20] H.Jégou, M.Douze, and C.Schmid. Improving bag-of-features for large scale image search. *IJCV*, 87(3):316–336, 2010. 2
- [21] H.Tamura, S.Mori, and T.Yamawaki. Textural features corresponding to visual perception. *IEEE Trans. Systems, Man and Cybernetics*, 8(6):460–473, 1978. 1
- [22] J.Han and K.K.Ma. Fuzzy color histogram and its use in color image retrieval. *TIP*, 11(8):944–952, 2002. 1
- [23] J.Ji, J.Li, S.Yan, B.Zhang, and Q.Tian. Super-bit locality-sensitive hashing. In *NIPS*, pages 108–116, 2012. 1
- [24] J.Philbin, O.Chum, M.Isard, J.Sivic, and A.Zisserman. Object retrieval with large vocabularies and fast spatial matching. In *CVPR*, pages 1–8, 2007. 6
- [25] J.Philbin, O.Chum, M.Isard, J.Sivic, and A.Zisserman. Lost in quantization: Improving particular object retrieval in large scale image databases. In *CVPR*, pages 1–8. IEEE, 2008. 4
- [26] J.Sivic and A.Zisserman. Video google: A text retrieval approach to object matching in videos. In *ICCV*, pages 1470–1477, 2003. 1, 2
- [27] J.Wang, H.T.Shen, J.Song, and J.Ji. Hashing for similarity search: A survey. *arXiv preprint arXiv:1408.2927*, 2014. 1
- [28] J.Wang, J.Wang, N.Yu, and S.Li. Order preserving hashing for approximate nearest neighbor search. In *ACM MM*, pages 133–142, 2013. 1
- [29] J.Wang, S.Kumar, and S.Chang. Semi-supervised hashing for large-scale search. *TPAMI*, 34(12):2393–2406, 2012. 1
- [30] K.Mikolajczyk and C.Schmid. A performance evaluation of local descriptors. *TPAMI*, 27(10):1615–1630, 2005. 1
- [31] L.Zheng, S.Wang, and Q.Tian. Coupled binary embedding for large-scale image retrieval. 2014. 2
- [32] L.Zheng, S.Wang, Z.Liu, and Q.Tian. Packing and padding: Coupled multi-index for accurate image retrieval. In *CVPR*, pages 1947–1954, 2014. 2
- [33] M.Datar, N.Immorlica, P.Indyk, and V.S.Mirrokn. Locality-sensitive hashing scheme based on p-stable distributions. In *SoCG*, pages 253–262, 2004. 1, 6, 14
- [34] M.K.Hu. Visual pattern recognition by moment invariants. *IRE Trans.Information Theory*, 8(2):179–187, 1962. 1
- [35] M.Norouzi and D.J.Fleet. Cartesian k-means. In *CVPR*, pages 3017–3024, 2013. 2
- [36] M.Patella, P.Ciaccia, and P.Zezula. M-tree: An efficient access method for similarity search in metric spaces. In *Proc. VLDB*, 1997. 1
- [37] N.Dalal and B.Triggs. Histograms of oriented gradients for human detection. In *CVPR*, volume 1, pages 886–893, 2005. 1
- [38] S.Weï, D.Xu, X.Li, and Y.Zhao. Joint optimization toward effective and efficient image search. *IEEE Trans. Cybernetics*, 43(6):2216–2227, 2013. 4, 5, 6
- [39] S.Weï, X.Wu, and D.Xu. Partitioned k-means clustering for fast construction of unbiased visual vocabulary. In *The Era of Interactive Media*, pages 483–493. 2013. 2
- [40] S.Weï, Y.Zhao, C.Zhu, C.Xu, and Z.Zhu. Frame fusion for video copy detection. *TCSVT*, 21(1):15–28, 2011. 2
- [41] W.Zhou, M.Yang, H.Li, X.Wang, Y.Lin, and Q.Tian. Towards codebook-free: Scalable cascaded hashing for mobile image search. *TMM*, 16(3):601–611, 2014. 1
- [42] W.Zhou, Y.Lu, H.Li, Y.Song, and Q.Tian. Spatial coding for large scale partial-duplicate web image search. In *ACM MM*, pages 511–520, 2010. 2

- [43] Y.Avrithis. Quantize and conquer: A dimensionality-recursive solution to clustering, vector quantization, and image retrieval. In *ICCV*, pages 3024–3031, 2013. [1](#)
- [44] Y.Jia, E.Shelhamer, J.Donahue, S.Karayev, J.Long, R.Girshick, S.Guadarrama, and T.Darrell. Caffe: Convolutional architecture for fast feature embedding. *arXiv preprint arXiv:1408.5093*, 2014. [2](#), [6](#)
- [45] Y.Sun, X.Wang, and X.Tang. Deep learning face representation from predicting 10,000 classes. In *CVPR*, pages 1891–1898, 2014. [2](#)
- [46] Y.Weiss, W.Xia, J.Huang, B.Ni, J.Dong, Y.Zhao, and S.Yan. CNN: Single-label to multi-label. *arXiv preprint arXiv:1406.5726*, 2014. [2](#)
- [47] Y.Weiss, A.Torralba, and R.Fergus. Spectral hashing. In *NIPS*, pages 1753–1760, 2009. [1](#)
- [48] Z.Liu, H.Li, W.Zhou, and Q.Tian. Embedding spatial context information into inverted filefor large-scale image retrieval. In *ACM MM*, pages 199–208, 2012. [2](#)
- [49] Z.Liu, H.Li, W.Zhou, R.Zhao, and Q.Tian. Contextual hashing for large-scale image search. 2014. [1](#)

A. Supplementary Material

In this supplementary material, we firstly discuss how multiple link (ML) number S and multiple assignment number W effect the image searching performance together. Then the experimental results and analyses on **Oxford** dataset, which are absent in regular paper, are given in the second section. Finally, we conduct experiments on three diverse and popular benchmarks under different settings to compare the proposed method with some hashing methods.

A.1. Interrelationship between ML and MA

A.1.1 Experimental Results of PQ+LSE

We conduct experiments under different combinations of S and W to evaluate the effect of multiple assignment and multiple link. The experimental results on **Holiday** and **Oxford** datasets are shown in Fig. 13 and Fig. 14 respectively. We set the binary embedding code length $L = 512$ and the threshold $T = 170$, the best value of factors.

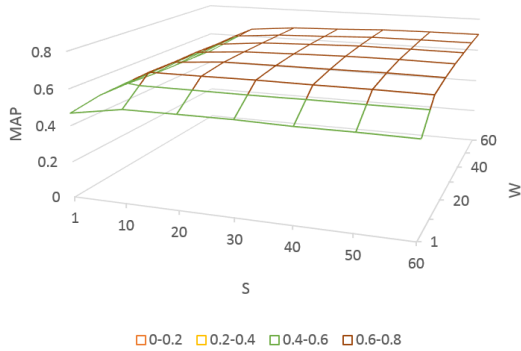


Figure 13. The accuracy interrelationship between S and W of PQ+LSE on **Holiday** dataset.

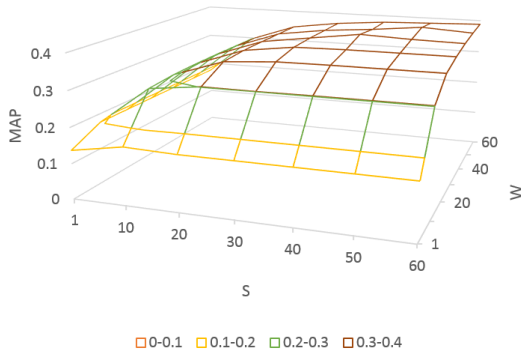


Figure 14. The accuracy interrelationship between S and W of PQ+LSE on **Oxford** dataset.

Clearly, when the value of S (or W) is fixed, the image searching accuracy is improved gradually with increasing the value of W (or S). The performance reaches the best

when the value of W (or S) goes up to value of S (or W). After that, the MAP score tends to be stable even increasing W (or S). The possible reason may lie in that the probability of finding correct images is biggest when $W = S$ as we have explained in the main paper. We summarize the observations as the two conclusions below:

Conclusion 1: When fix the ML number S (or the MA number W), the MAP value increases with the growth of MA number W (or the ML number S).

Conclusion 2: When $W = S$, we can get the best trade-off, and a relative larger value of $W = S$ can reach the higher accuracy.

A.1.2 Experimental Results of TF+LSE

Similar conclusions can be got from TF+LSE scheme. The experimental results on two benchmarks are illustrated in Fig. 15 and Fig. 16. However, there is a little difference between PQ+LSE and TF+LSE schemes. For TF+LSE scheme, the best performance cannot be obtained at the $W = S$ condition, since the link strategy of TF+LSE is depended on the descriptiveness of CNN components. In fact, when S goes up to large value (e.g, 24), the performance tends to be stable. This means that the top 24 components of CNN feature mostly describe an image. The choice of W can be larger than S . When S is fixed, searching accuracy is improved with the growth of W . The performance tends to be stable when W goes up to large value (e.g, 45).

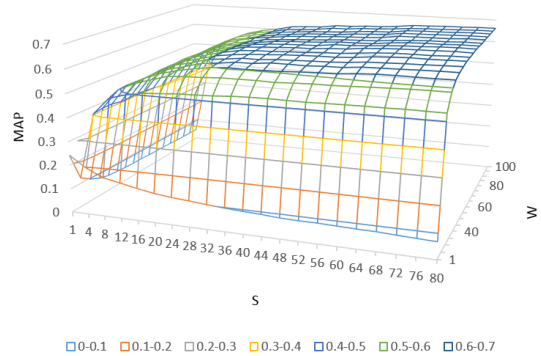


Figure 15. The accuracy interrelationship between S and W of TF+LSE on **Holiday** dataset.

A.2. Experimental Results on Oxford Dataset

In this section, we show the experimental results on **Oxford** dataset.

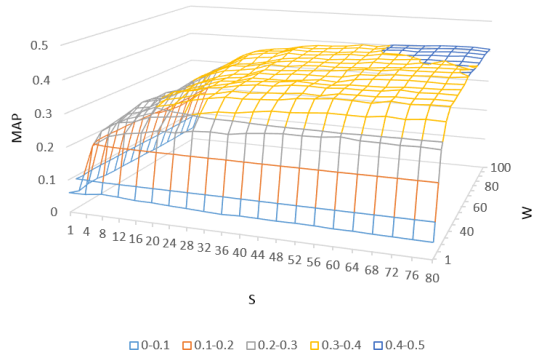


Figure 16. The accuracy interrelationship between S and W of TF+LSE on **Oxford** dataset.

A.2.1 Effect of Key Parameters

The effort of factor L on **Oxford** dataset is shown in Fig. 17. Clearly, the code with medium length performs best, which is consistent with the conclusion from **Holiday**. This also means that the factor L is not sensitive to various datasets. Therefore, we set $L = 512$ in the following experiments.

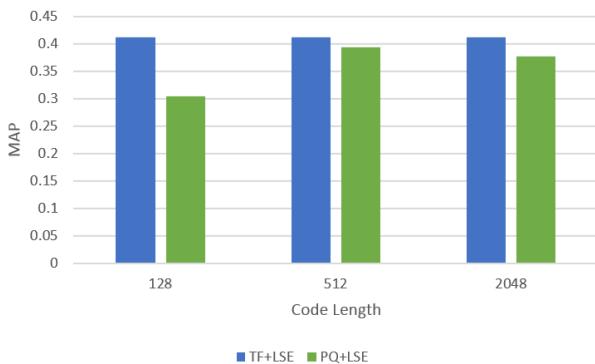


Figure 17. The sensitivity of factor L on **Oxford** dataset.

To test the sensitivity of distance threshold T , we perform the same experiments on **Oxford** dataset. The experimental results are illustrated in Fig. 18. The curve is effected by the distribution of correct images corresponding to threshold, and the rising part of the curve contains correct images. In TF+LSE scheme, correct images distribute in the scope where $T \leq 80$. While in PQ+LSE scheme, the scope is the combine of $T \leq 90$ and $120 \leq T \leq 170$. The best performance reaches at $T = 170$ in both schemes, and it fits the rule of threshold.

For the factors S and W of PQ+LSE, we force them to be equal according to the conclusions from Section A.1.1. The experimental results are illustrated in Fig. 19 and Fig. 20. Different from **Holiday** dataset, the best performance reaches when S and W are equal to 50. This is reasonable because the optimal S is depend on the distribution of true

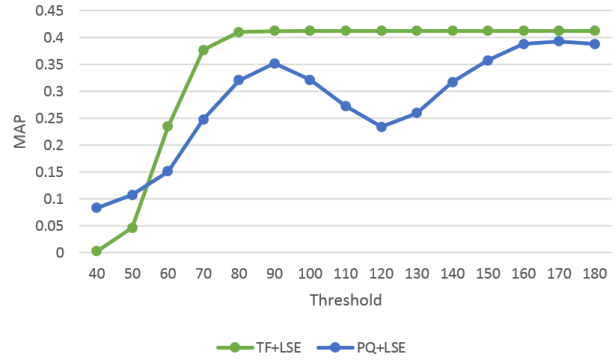


Figure 18. The sensitivity of factor T on **Oxford** dataset.

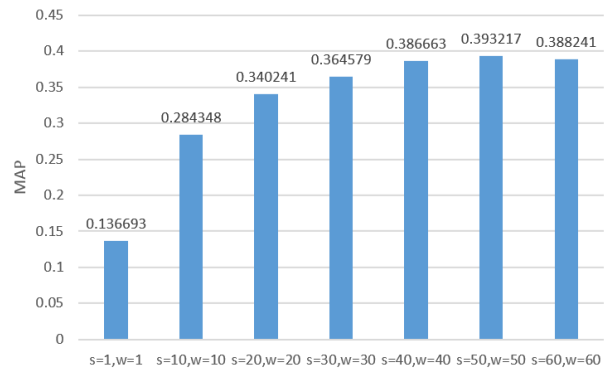


Figure 19. The accuracy sensitivity of factor S and W on **Oxford** dataset.

relevant images. When the true relevant images are centralized, a bigger factor is proper since the possibility that they are assigned to the same S nearest visual words is big. Since the distribution of true relevant images in **Oxford** are relatively scattered, the optimal value of S is relatively smaller.

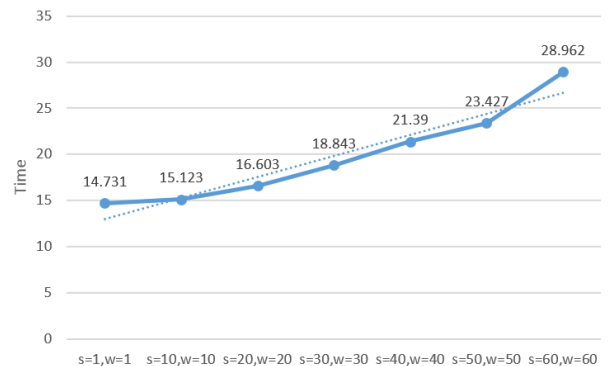


Figure 20. The speed sensitivity of factor S and W on **Oxford** dataset.

The sensitivity of R is tested on M-PQ+LSE scheme. The results are shown in Fig. 21 and Fig. 22. When $R < 11$ the MAP score increases obviously with R , while when

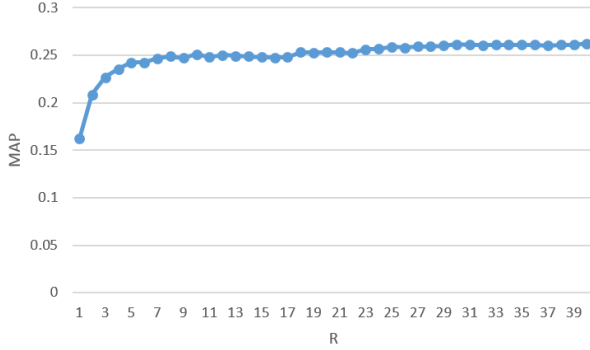


Figure 21. The accuracy sensitivity of factor R on **Oxford** dataset.

$R \geq 11$ the score tends to be equal. The time cost increases linearly with R , which is consistent with the experimental results on **Holiday** dataset.

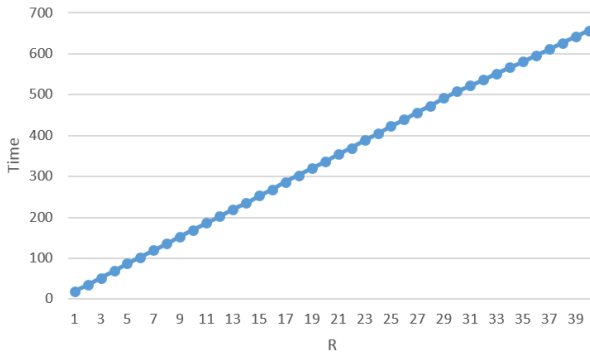


Figure 22. The speed sensitivity of factor R on **Oxford** dataset.

A.2.2 Comparison of Different Schemes

The comparison results of various schemes on **Oxford** dataset are shown in Table 4-6. For testing the real performance of schemes, there is no optimization in all program codes. Different from **Holiday** dataset, **Oxford** and **Flickr1M** are both from Flickr [2] website. When building inverted table on large scale dataset, we observe that many distractor set images are linked to the same bins with landmark set images. It makes the search time of a query much longer than on **Holiday** dataset. Here we choose the sub-optimal factors which makes the time cost acceptable.

For TF+LSE scheme, we set $S = 24, W = 45$ for the balance of accuracy and speed. For PQ+LSE scheme, the search time mainly depends on the factor W , and any value bigger than 10 is not acceptable since an inverted table bin is linked with too many images. Here we set $S = 10, W = 10$ for the best trade-off. Indeed, as shown in Fig. 14 and 16, both two schemes can perform a better performance than the baseline. But on large scale dataset, the search time

also approaches the baseline, which is not prosper. For M-PQ+LSE scheme, speed is mainly depended on R . We choose $R = 11$, a proper value according to the change curve in Fig. 21.

Table 4. Evaluation of Searching Accuracy on **Oxford**.

Method	Dataset	
	Oxford	Oxford+Flickr1M
BF (baseline)	0.361740	0.347725
TF+LSE	0.344364	0.334408
PQ+LSE	0.284348	0.283678
M-PQ+LSE	0.248202	0.260936
TF+PQ+LSE	0.375635	0.366803

Table 5. Evaluation of Search Time on **Oxford**. (Unit: s)

Method	Dataset	
	Oxford	Oxford+Flickr1M
BF (baseline)	9.359	1667.166
TF+LSE	2.151	8.070
PQ+LSE	16.429	82.115
M-PQ+LSE	154.627	186.12
TF+PQ+LSE	19.209	106.725

As shown in Table 4 and Table 5, our proposed schemes make a balance with accuracy and speed. More importantly, the searching time is sub-linear with the growth of dataset. Besides, even on the sub-optimal case, the TF+PQ+LSE scheme which combines TF+LSE and PQ+LSE, still outperforms the baseline. The long search time of PQ+LSE is mainly because the landmark and distractor sets are mingled in the feature space, and each bin of inverted table is linked with too many images. A better training set or a balanced link strategy can solve this problem.

Table 6. Evaluation of Storage Usage on **Oxford**. (Unit: MB)

Method	Dataset	
	Oxford	Oxford+Flickr1M
BF (baseline)	79.09	14141.59
TF+LSE	72.34	1555.50
PQ+LSE	18.91	602.56
M-PQ+LSE	175.49	817.50
TF+PQ+LSE	91.25	2158.06

The memory usage of each scheme is shown in Fig. 6, which is also sub-linear with the dataset size. For huge dataset, the memory usage of all proposed schemes is much smaller than the baseline. When dataset becomes larger, the proposed schemes only need more space to store inverted table items, which are much smaller than features.

A.3. Compared with LSH

In this section, we compare PQ+LSE scheme with Locality Sensitive Hashing (LSH) [33], an effective hashing scheme. For more general comparison, **UKbench** dataset is added as the third landmark.

UKbench [10] is a dataset of 10,200 images. Each 4 images are in a group, which are the photos of the same object from different viewpoints. The first image of each group is collected as a query set, which contains 2550 images in total.

Table 7. Evaluation of Searching Accuracy Compared with LSH.

Dataset	Method		
	BF	PQ+LSE	LSH
Holiday	0.788241	0.702020	0.777724
Holiday+Flickr1M	0.788205	0.701414	0.775665
Oxford	0.361740	0.284348	0.206599
Oxford+Flickr1M	0.347725	0.283678	0.181309
UKbench	0.802275	0.798822	0.524177
UKbench+Flickr1M	0.797425	0.793721	0.504802

The searching accuracy comparison between PQ+LSE and LSH is shown in Table 7, BF scheme is still treated as the baseline. We set the code length to 512 and both schemes are trained from the same training set. From Table 7 we can observe that PQ+LSE scheme are more robust than LSH. On all three benchmarks, the performance of PQ+LSE is close to the baseline, while the performance of LSH is quite different on benchmarks. Generally speaking, using only LSH scheme will lead to large quantization error and decrease the search accuracy. The special case is the performance on **Holiday** dataset, on which the LSH scheme outperforms the PQ+LSE scheme. The possible reason lies in the distribution of true relevant images. For **Holiday** dataset, the queries and their true relevant images are centralized closely, relevant images can be returned with a higher probability by using LSH scheme. In addition, LSH is effected strongly by the training set. Since LSH needs to calculate a mean vector from the training set to normalize the feature vectors, the quality of the mean vector affects the performance of LSH. But PQ+LSE uses training set to train the codebook of inverted table, which is more robust with the training set.